Ketone Photolysis in the Presence of Oxygen: A Useful Source of OH for Flash Photolysis Kinetics Experiments

S. A. CARR, M. T. BAEZA-ROMERO, M. A. BLITZ, B. J. S. PRICE, P. W. SEAKINS

School of Chemistry, University of Leeds, Leeds, LS2 9JT, UK

Received 12 April 2007; revised 10 July 2007, 11 January 2008; accepted 12 February 2008

DOI 10.1002/kin.20330
Published online in Wiley InterScience (www.interscience.wiley.com).

ABSTRACT: Previous studies have shown a significant OH yield from the reaction of RCO radicals (generated from the photolysis of corresponding ketone) with oxygen below total pressures of 200 Torr. The potential of these reactions as a source of OH radicals for flash photolytic kinetic studies is investigated. The viability of the method was tested by measuring rate coefficients for the reaction of OH with ethanol using both acetone/O_2 mixtures and *t*-butyl hydroperoxide photolysis. The results (with statistical errors at the 2σ level) are in excellent agreement with each other (k_{EtOH}(acetone) = (5.87 ± 0.34) × 10^{-18} T^2 exp((515 ± 21)K/T) cm^3 $molecule^{-1}$ s^{-1} and k_{EtOH} (*t*-butyl hydroperoxide) = (5.27 ± 0.34) × 10^{-18} T^2 exp((557 ± 20)K/T) cm^3 $molecule^{-1}$ s^{-1}) and with the IUPAC recommendation. The reaction of OH with methyl ethyl ketone (2-butanone) has also been investigated using a similar technique. The results show a strong non-Arrhenius temperature dependence, k = (3.84 ± 0.12) × 10^{-24}× T^4 × exp((1038 ± 11)/T). The merits of the ketone/oxygen OH source are contrasted with other established precursors. A major advantage of the technique is the ability to cleanly generate OD without the potential for isotopic scrambling prior to photolysis. © 2008 Wiley Periodicals, Inc. Int J Chem Kinet 40: 504–514, 2008

INTRODUCTION

The hydroxyl radical (OH) is a crucial intermediate in both atmospheric [1] and combustion chemistry [2]. Attack by OH radicals is often the dominant removal process for organic material in the atmosphere and as such, OH chemistry controls the lifetimes (τ) of such species in the atmosphere.

$$\tau = \frac{1}{k_{bi}[OH]_{av}} \quad \text{(E1)}$$

where k_{bi} is the bimolecular rate coefficient and $[OH]_{av}$ is the average OH concentration. Similarly in combustion, fuel removal is dominated by reactions of OH radicals. The importance of the OH radical is reflected in the number of kinetic measurements

Correspondence to: P. W. Seakins; e-mail: p.w.seakins@leeds.ac.uk.
Contract grant sponsor: EPSRC.
Contract grant number: GR/T28560/01.

performed over the years, with the NIST database (http://kinetics.nist.gov) listing more than 1000 OH reactions. Despite the depth of study, many important reactions remain to be measured. For example, the master chemical mechanism [3], a comprehensive model for the oxidation of more than 120 organic compounds, has several thousand OH abstraction reactions. Also, additional measurements are required to broaden the range of conditions for previously studied reactions. Both discharge flow and laser flash photolysis have been used in the study of OH kinetics. Each technique has its advantages and disadvantages, and complementary studies by both technique give confidence that systematic errors are absent. However, flash photolysis has significant advantages in that much wider ranges of temperatures and pressures can be studied.

In this paper, we discuss the merits of ketone photolysis (R1a) with subsequent reaction of the RCO fragment with oxygen (R1b) as a convenient OH source.

$$\mathrm{RCOR} + h\nu \rightarrow \mathrm{RCO} + \mathrm{R} \qquad \text{(R1a)}$$

$$\mathrm{RCO} + \mathrm{O_2} \rightarrow \mathrm{OH} + \text{coproducts} \qquad \text{(R1b)}$$

A number of different sources have been used in previous flash photolysis studies, and before discussing the merits of the current source, we briefly review other commonly used sources.

Hydroperoxides

Hydroperoxides, either H_2O_2 or organic peroxides ROOH, have a number of useful advantages: They have significant cross sections at common excimer and YAG wavelengths (see Fig. 1), produce ground state OH in its lowest vibrational level cleanly from the dissociation of the weak peroxide bond and, for H_2O_2, without any other coproduct at 248 nm [4,5]. However, peroxides pose some significant handling problems; because of their explosive nature, they are usually available only as a solution. Either further purification is required or the experimenter must be resigned to having water in the system. At higher temperatures, the peroxides will thermally decompose and at low temperatures condensation can occur. The presence of the OH group means that deuterated peroxides can exchange H and D, and hence production of pure OD in the absence of OH may be a problem.

Nitrous Acid

A common precursor used for long-wavelength photolysis is nitrous acid (HONO) due to absorption in a diffuse structured band between 300 and 390 nm

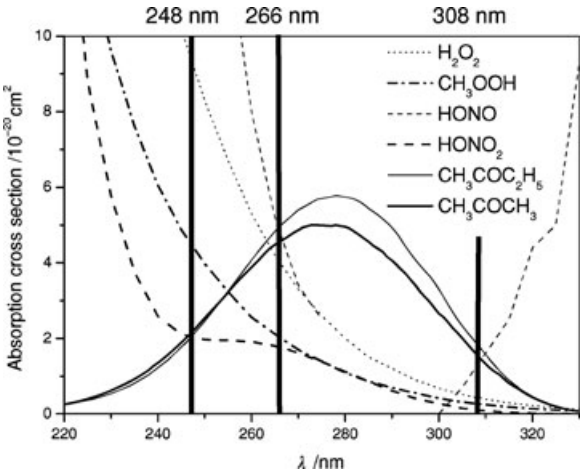

Figure 1 Absorption cross sections of common OH precursors from IUPAC recommendations [9]. The solid vertical lines show common laser photolysis wavelengths in this region.

(Fig. 1). For example, photolysis at 351 nm (using a XeF excimer laser) was used to study OH + ketones as the threshold frequency for ketone photolysis is around 340 nm [6,7]. Relatively unreactive NO is produced as a coproduct. There is a possible complication due to channel (2b) producing H atoms, but Wollenhaupt et al. [8] showed channel (2b) to be less then 1% at 351 nm.

$$\mathrm{HONO} + h\nu \rightarrow \mathrm{HO} + \mathrm{NO} \quad \lambda_1 = 578\ \mathrm{nm} \qquad \text{(2a)}$$

$$\mathrm{H} + \mathrm{NO_2} \quad \lambda_2 = 361\ \mathrm{nm} \qquad \text{(2b)}$$

Kinetics at temperatures up to 725 K has been performed [6] without influence from any HONO decomposition. Nitrous acid is not commercially available, and other forms of NO_x may be present in the sample. Again, the presence of the OH moiety means that isotope exchange may be an issue.

Nitric Acid

Both normal and deuterated nitric acid ($HONO_2$) can be obtained cheaply, although purification is required to remove other nitrogen oxides. Nitric acid has a large cross section at short wavelengths (Fig. 1); unfortunately, a number of photolysis channels are open at these wavelengths (reactions (3a)–(3f)), where the wavelength given corresponds to the thermodynamic limit.

$$\mathrm{HONO_2} + h\nu \rightarrow \mathrm{HO} + \mathrm{NO_2}(\mathrm{X^2A_1}) \quad \lambda_{3a} = 604\ \mathrm{nm} \qquad \text{(3a)}$$

$$HONO + O(^3P) \qquad \lambda_{3b} = 393 \text{ nm} \tag{3b}$$

$$HO + NO_2(1^2B_2) \qquad \lambda_{3c} = 381 \text{ nm} \tag{3c}$$

$$H + NO_3 \qquad \lambda_{3d} = 278 \text{ nm} \tag{3d}$$

$$HONO + O(^3P) \qquad \lambda_{3e} = 242 \text{ nm} \tag{3e}$$

$$HONO(a^3A'') + O(^3P)\lambda_{3f} = 216 \text{ nm} \tag{3f}$$

IUPAC currently recommends that the OH-forming channels ((R3a) and (R3c)) account for more than 97% of the products at 248 nm but only 90% and 33% at 222 and 193 nm, respectively [9]. At longer wavelengths where the production of OH is the dominant process, the absorption cross section of $HONO_2$ is relatively small as can be seen in Fig. 1. Once again the OH grouping may cause difficulties in mechanistic studies based on clean OD generation.

At 248 nm, a small amount of OH is produced vibrationally excited ($\sim$1% in $v = 1$ and 0.4% in $v = 2$) [10]. Some studies require the production of vibrationally excited species, for example, as a probe for the high-pressure association limit [11], but in other cases the vibrational cascade from significantly populated upper levels could cause complications.

$O(^1D)$ + Hydrogen Source

Nitrous oxide (N_2O) photolysis at 193 nm cleanly generates excited oxygen atoms, $O(^1D)$ [12], which can react very rapidly with hydrogen-containing species (typical rate coefficients in the order of 1×10^{-10} cm^3 molecule^{-1} s^{-1}) inserting into bonds and releasing OH from the decomposition of the chemically activated molecule. For example,

$$O(^1D) + CH_4 \rightarrow CH_3OH^* \rightarrow CH_3 + OH(v) \tag{R4}$$

$$O(^1D) + H_2O \rightarrow HOOH^* \rightarrow 2OH(v) \tag{R5}$$

Ozone photolysis at 248 nm can also be used as the $O(^1D)$ source. OH is generated in a range of vibrational levels with the precise distribution being dependent on the hydrogen source. When water is used as the hydrogen source then the vibrational distribution is bimodal [13]. Although the production of vibrationally excited species may be a possible disadvantage for thermal studies, the method has been used to good effect by Hynes and coworkers [14,15] and Yamasaki et al. [16] to study vibrational relaxation in OH. If all the $O(^1D)$ is not intercepted by the hydrogen source, then quenching can occur to give ground state oxygen atoms, $O(^3P)$, which may be a long-time source of OH.

The major advantage of the method is the very high thermal stability of the N_2O precursor, and if hydrogen or methane is used as the hydrogen source then isotope exchange is very limited. However, nitrous oxide photolysis is limited to wavelengths below 200 nm, where photolysis of some substrates could cause complications. Ozone generation is not without complications and is thermally unstable.

This paper focuses on an alternative method for generating OH radicals as generically introduced in reaction (1) above and discussed here for the acetyl radical. The first step in the reaction is the formation of the excited peroxy species:

$$CH_3CO + O_2 \rightarrow CH_3CO(O_2)^* \rightarrow OH + \text{products} \tag{R6a}$$

$$\downarrow [M] \tag{R6b}$$

$$CH_3CO(O)_2$$

Either the peroxy radical can be collisionally stabilized or alternatively an internal abstraction can take place with the production of OH [17–19]. The exact nature of the coproducts is uncertain [20]. Formaldehyde + CO or a three-membered lactone appear to be the most likely products. The first observation of OH production was made by Michael et al. [17] who showed that OH regeneration was almost complete following the reaction of OH with acetaldehyde at low pressures in the presence of oxygen. There have been several determinations of the yield of OH from reaction (6a) [18,19,21–23] and while there is some controversy as the absolute yield, all groups report significant OH yields at pressures below 50 Torr.

Acetyl radicals can be generated from a number of precursors either by photolysis or by chemical reaction (e.g., $Cl + CH_3CHO \rightarrow CH_3CO + HCl$); however, for the kinetic studies described in this paper ketone photolysis is the most relevant source. Figure 1 shows that ketone photolysis extends into the near UV. In this region ketone photolysis occurs with the fragmentation of a single carbon–carbon bond,

$$R'COR'' + h\nu \rightarrow R'CO + R'' \tag{R7a}$$

$$\rightarrow R''CO + R' \tag{R7b}$$

Depending on the wavelength of photolysis and the pressure, the RCO fragment may dissociate further to give an alkyl radical and carbon monoxide. At 193 nm,

all the CH_3CO formed from acetone photolysis dissociates, although studies of the rotational distribution of the CO product indicate that the dissociation is still sequential [24]. Somnitz et al. [25] have studied the photolysis of acetone at 248 nm where the quantum yield for CO formation (as measured by IR diode laser spectroscopy) decreases from ~0.45 at 20 mbar to ~0.25 at 900 mbar showing that at this wavelength unimolecular decomposition of the excited CH_3CO fragment is in competition with stabilization. Longer wavelength photolysis will deposit less energy into the CH_3CO fragment and less dissociation of the acetyl will occur. Additionally, at long wavelengths, the pressure and temperature dependence of the primary quantum yield needs to be considered [26].

Issues surrounding ketone photolysis and the OH yield from the acetyl + O_2 reaction will be more fully discussed in forthcoming papers. In this study, we focus on mapping out the conditions under which ketone photolysis in the presence of oxygen is a useful OH source. To confirm the validity of the method, we compare measured rate coefficients for the reaction of OH with ethanol (R8) and with methyl ethyl ketone (MEK; R9) with OH being generated from *t*-butyl hydroperoxide photolysis (*t*-C_4H_9OOH) and ketone/O_2.

$$OH + C_2H_5OH \rightarrow \text{products} \qquad \text{(R8)}$$

$$OH + CH_3COC_2H_5 \rightarrow \text{products} \qquad \text{(R9)}$$

EXPERIMENTAL

All reactions were carried out in a conventional slow flow laser flash photolysis apparatus. The OH precursor(s), substrate, and helium buffer gas were premixed in a mixing manifold before being flowed through the reaction cell. The cell was a metal, six-way cross design with the photolysis and OH probe lasers being directed along perpendicular baffled arms into a central reaction zone. Fluorescence was observed by a photomultiplier mounted mutually perpendicularly to the two laser beams.

Gases were flowed through calibrated mass flow controllers, and the pressure in the cell was controlled by a needle valve mounted in the exhaust line. Flow rates were chosen to ensure a fresh sample of gas in the photolysis region for each photolysis pulse (typically the laser repetition rate was 5 Hz). During experiments, the pressure in the cell was monitored by a capacitance monometer (Leybold Vacuum, 0–100 Torr and MKS, >100 Torr). The cell could be evacuated by a diffusion pump to $<10^{-5}$ Torr overnight. Two different cells were used for subambient and high-temperature experiments. For the subambient studies, the cell was mounted in a stainless steel bath containing a thermal fluid (Huber DW-Therm-90 $\cdots$ 200°C) cooled by an immersion probe (Lab Plant). For high-temperature work the central portion of the cell was heated by Watlow cartridge heaters mounted in the body of the cell. In both cases, the temperature in the central portion of the cell, where the photolysis and probe lasers intersect, was measured with a K-type thermocouple.

Acetone (99%+), *t*-butyl hydroperoxide (Sigma-Aldrich, Gillingham, UK; 70% aq.), ethanol (Aldrich, Poole, UK; ≥99.5% (200 proof)), and MEK (Aldrich; 99.5+%) were purified by several freeze–pump–thaw cycles. He (BOC Guildford, UK; CP grade, 99.999%) and O_2 (Air Products; Walton-on-Thames, UK; high purity, 99.999%) were used without further purification.

OH radicals were generated by pulsed laser photolysis (~10–20 mJ $pulse^{-1}$ with a photon density of (5–10) × 10^{15} photons cm^{-1} s^{-1}) of a suitable precursor at 248 nm in typical concentrations of (1–5) × 10^{11} molecule cm^{-3}. OH radicals were probed using off resonance laser induced fluorescence. Probe light, corresponding to excitation to $v = 1$ in the first excited state was generated from a frequency doubled, pulsed NdYAG (Spectra-Physics, Quanta-Ray GCR 100-series) pumped dye laser (Spectra-Physics, Quanta-Ray PDL-3) operating with Rhodamine 6G dye generating light at approximately 564 nm. This light was then frequency doubled and the laser tuned to match the energy of the OH ($A^2\Sigma(v = 1) \leftarrow X^2\Pi(v = 0)$, $Q_1(1)$) transition at ~281.9 nm. Off resonance fluorescence was collected by a quartz lens and focused onto a photomultiplier tube (PMT) (B2F/RFI Thorn EMI electron tubes) through a 308-nm filter (Melles Griot, 310 nm, FWHM = 10 ± 2 nm). The output from the PMT was collected via a boxcar integrator, digitized and stored for subsequent analysis on a PC. The firing of the photolysis and probe lasers was controlled by a delay generator, and a program was written to vary the time interval between the photolysis and probe lasers. Negative delays correspond to a pretrigger baseline. Typically each datum point for traces such as those shown in Fig. 2 was the mean of 2–4 laser pulses.

The concentrations of substrate gases were always greatly in excess of the OH, ensuring that OH decayed with pseudo-first-order kinetics. Under these conditions the OH signal, S, when C_4H_9OOH was used as the source could be described by a single exponential decay (Fig. 2):

$$S_{OH}(t) = S_{OH}(0)\, e^{-k't} \qquad \text{(E2)}$$

where k' is the pseudo-first-order rate coefficient given by

$$k' = k_{bi}[\text{substrate}] + k_{diff} \qquad \text{(E3)}$$

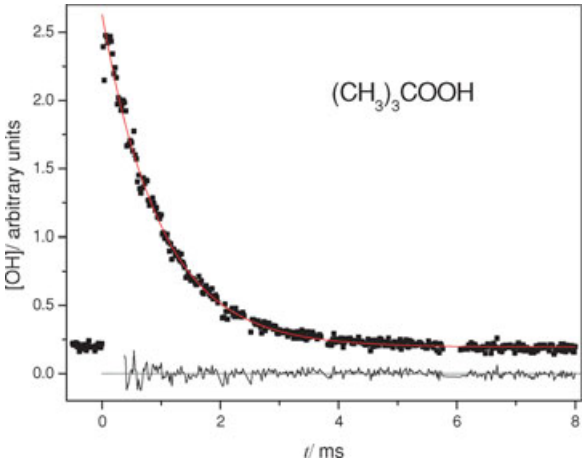

Figure 2 Typical OH temporal profile for the reaction of OH with ethanol with C_4H_9OOH as the precursor (T = 298 K, total pressure = 200 Torr He, [EtOH] = 2.3×10^{14} molecule cm^{-3}, [t-C_4H_9OOH] = 8.5×10^{13} molecule cm^{-3}). The two rising points following photolysis are the delayed response of the PMT following gating. The estimated initial OH concentration is $\sim 1 \times 10^{11}$ molecule cm^{-3}.

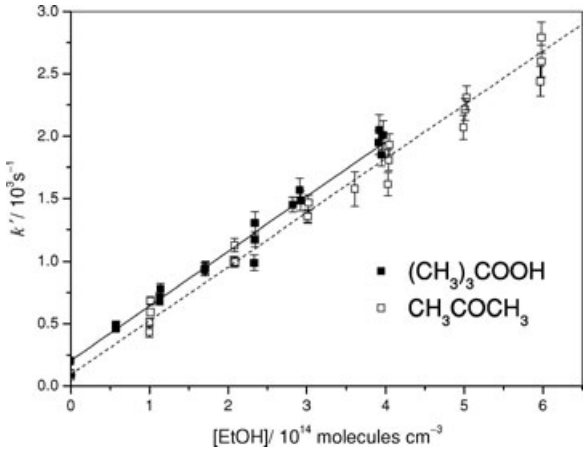

Figure 3 Bimolecular plot for reaction (8) at 500 K and a total pressure of 50 Torr He, showing data from both OH sources. The solid line shows a least-squares linear fit to the t-C_4H_9OOH precursor data (■), k' (s^{-1}) = (4.37 ± 0.10) × 10^{-12} × [EtOH] + (205 ± 8), and the dotted line shows a least-squares linear fit to the acetone precursor data (□), k' (s^{-1}) = (4.32 ± 0.15) × 10^{-12} × [EtOH] + (93 ± 5).

where k_{bi} is the desired bimolecular rate coefficient and k_{diff} represents the sum of pseudo-first-order loss processes due to diffusion from the observation region and reaction with the precursor. Decay traces were fitted using a nonlinear least-squares programme to yield k'. To extract the bimolecular rate coefficient, decays were recorded as a function of substrate concentration at a fixed precursor concentration. A typical bimolecular plot is shown as the full lines in Fig. 3 for the reaction of OH with ethanol, where the error bars on the data points represent the statistical error (2σ) from the fitting process. The bimolecular rate coefficient is the gradient of the plot and was extracted from a weighted linear least-squares fit. The statistical errors in the bimolecular rate coefficients can be combined in quadrature with an estimated additional 10% uncertainty arising from errors in flow controllers, bulb manufacture, and pressure readings.

When a ketone/oxygen system was used to generate OH, the OH profiles showed a rapid growth and subsequent decay, as illustrated in Fig. 4. Solution of the rate law for OH with production from reaction (6a) and removal due to reaction with the substrate yields a biexponential expression (E4):

$$[OH]_t = \frac{\alpha[CH_3CO]_0 k'_6}{(k'_6 - k'_s)}(\exp(-k'_s t) - \exp(-k'_6 t)) \quad \text{(E4)}$$

where α represents the fraction of (R6) going via (R6a), k' represents the pseudo-first-order rate coefficient, $k'_6 = k_6[O_2]$, $k'_s = k_{bi}$[substrate] + k_{diff} and $[CH_3CO]_0$ is the initial acetyl concentration. Equation (E4) was used to fit the experimental data to extract pseudo-first-order rate coefficients for reaction of OH with substrate.

Oxygen concentrations were such that the growth was rapid compared to the decay. When the growth was extremely rapid, the first few points of the OH profile could be ignored and the remaining decay analyzed by a simple exponential.

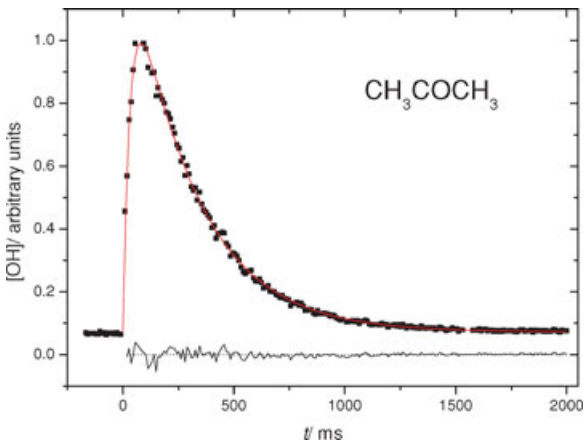

Figure 4 Typical OH temporal profile for the reaction of OH with ethanol with acetone/O_2 as the OH precursor (T = 298 K, pressure 25 Torr He, [O_2] = 2.3×10^{16} molecule cm^{-3}, [acetone] = 1.1×10^{14} molecule cm^{-3}, [C_2H_5OH] = 9.77×10^{13} molecule cm^{-3}). The maximum OH concentration is estimated to be $\sim 1 \times 10^{11}$ molecule cm^{-3} for this experiment.

The dashed lines on Fig. 3 show a bimolecular plot obtained using the ketone/oxygen system. Note also that the intercept in Fig. 3 is significantly lower for the acetone precursor experiments. Comparable concentrations of precursor are used in both experiments, but the room temperature rate coefficient for OH reaction with acetone [6,9] is approximately a factor of 20 below that for *t*-butyl hydroperoxide [27].

RESULTS

OH + C_2H_5OH

The results of this reaction from 298 to 500 K are presented in Table I and are compared with previous studies in Fig. 5. Above 500 K, OH regeneration from the decomposition of one of the reaction pathways becomes significant; observed in this study and also reported by Hess and Tully [28]. The studies were carried out over a wide range of pressures and as expected for a hydrogen abstraction reaction, no significant variations in the measured rate coefficients as a function of pressure were observed. Variations in laser repetition (factor 5) and flow rates (factor 3) were also undertaken to check for effects of secondary reactions or loss of substrate; again no significant effects were observed.

For comparison, the data were separately fitted to a three-parameter expression of the form $k = AT^2\exp(B/T)$ for comparison to the IUPAC data and the results are presented in Table II with first the data weighted $(1/(\text{error})^2)$ solely by the statistical errors in the bimolecular rate coefficients and second weighted by the estimated total error (the statistical error and an estimated 10% systematic error combined in quadrature). The reported errors represent the 95% confidence limits from the fitting procedures with the appropriate student *t* value. These values agree extremely well with each other in spite of the small data set. Good agreement is also seen with the current IUPAC recommendation [29] for this reaction, $k_{\text{EtOH}} = 6.7 \times 10^{-18}\ T^2\ \exp(511\text{K}/T)\ \text{cm}^3\ \text{molecule}^{-1}\ \text{s}^{-1}$, which is based on the studies of Wallington and Kurylo [30], Hess and Tully [28], Jimenez et al. [31], and Dillon et al. [32]. The results at room temperature are well within the 20% uncertainty (at room temperature) of the evaluation [29]. Given that many of the systematic errors will cancel out in our studies, data and parameterizations based on statistical errors are most relevant for comparisons of the two precursors, whereas the parameterization based on the total estimated error should be used to compare with the IUPAC evaluation.

OH + $CH_3COC_2H_5$

The reaction of OH with MEK has been determined over a wide range of temperatures (213–598 K). For these studies photolysis of the ketone itself has been used as one of the precursors. Two photolysis channels are possible: $CH_3CO + C_2H_5$ and $C_2H_5CO + CH_3$, with the former channel predicted to dominate on thermodynamic grounds. However, from the point of view of an OH source, there is relatively little difference

Table I Summary of Results for the OH + C_2H_5OH Reaction (R8)

T (K)	*P* (Torr)	k (10^{-12} cm^3 molecule^{-1}s^{-1})[a]	[EtOH] (10^{14} molecule cm^{-3})	[Precursor] (10^{14} molecule cm^{-3})	[O_2] (10^{16} molecule cm^{-3})	[OH]$_0$ (10^{11} molecule cm^{-3})[b]
			t-Butyl hydroperoxide			
298	25	3.16 ± 0.03	1.1–8.6	2.7	–	4.3
298	198.1	2.93 ± 0.03	1.1–8.2	0.85	–	1
378	25.01	3.12 ± 0.05	1.2–8.5	0.65	–	0.75
378	198.5	3.15 ± 0.11	1.5–11	0.21	–	0.2
500	25	4.32 ± 0.10	1.1–7.7	0.15	–	0.2
500	50.2	4.06 ± 0.24	1.0–7.4	0.27	–	0.4
			Acetone			
298	25.1	2.91 ± 0.07	1.8–13	1.9	7.0	1.5
298	49.9	2.99 ± 0.05	1.7–11	3	7.1	2
378	24.9	3.25 ± 0.07	1.6–8.9	2.1	3.1	1.8
378	25.3	3.02 ± 0.09	1.2–8	3	3.9	2.5
378	49.9	3.31 ± 0.07	1.1–8.9	2.5	3.2	2.1
498	25.2	4.37 ± 0.15	0.57–3.9	1.6	2.3	0.75
498	50	4.10 ± 0.08	0.8–8.9	1.2	1.8	0.56

[a] Errors are 2σ statistical errors from the weighted linear fits of the pseudo-first-order rate coefficient vs. [EtOH].
[b] Maximum [OH] were estimated using the absorption cross section recommended by IUPAC [9] at 248 nm for CH_3OOH.

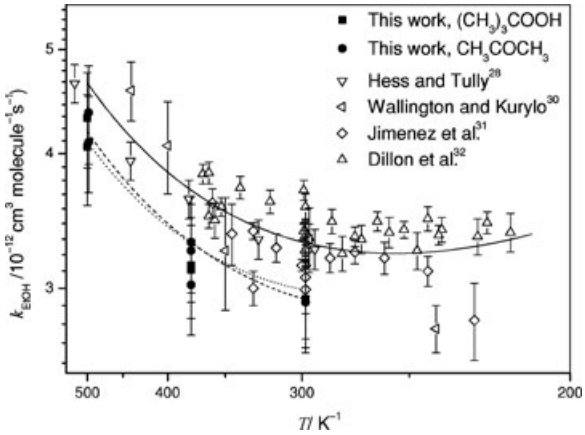

Figure 5 Temperature dependence of reaction (8). The dotted line is the fit to our data with acetone as a precursor, the dashed line is the fit to our data with *t*-butyl hydroperoxide as the precursor, and the solid line is the IUPAC recommendation [29] which has an uncertainty of ∼20%.

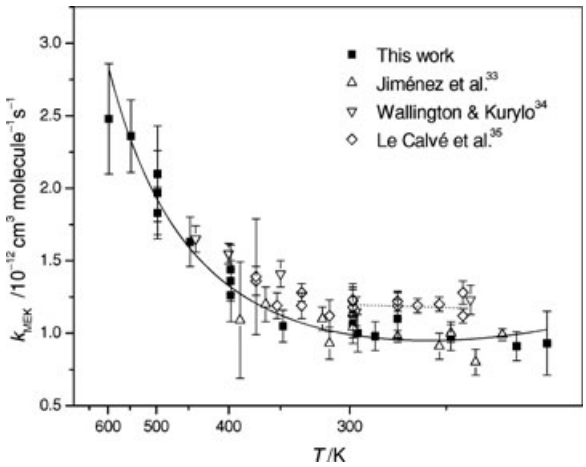

Figure 6 Temperature dependence of the rate coefficient for reaction (9). Data: (■); this work, (△); Jimenez et al. [33], (▽); Wallington and Kurylo [34], (◇); Le Calve et al. [35]. The dotted line is the IUPAC recommendation ($1.3 \times 10^{-12} \times \exp(-25/T)$ cm^3 $molecule^{-1}$ s^{-1}) [29]. The solid line is a fit to our experimental data.

as previous work in the laboratory has shown that the $C_2H_5CO + O_2$ reaction also generates OH with a significant yield at low pressures [23]. The results of the current studies are summarized in Table III and compared with other work in Fig. 6. The present results give a modified Arrhenius temperature dependence, $k = AT^n \exp(-E/RT)$, given by, $k_{MEK} = (3.84 \pm 0.12) \times 10^{-24} \times T^4 \times \exp((1038 \pm 11)/T)$ weighted only with statistical errors from the bimolecular rate coefficients and $k_{MEK} = (3.94 \pm 0.42) \times 10^{-24} \times T^4 \times \exp((1031 \pm 35)/T)$ with a weighting based on the statistical error and an estimated 10% systematic error combined in quadrature. In each case, the parameters are obtained by first fitting the data with a weighted fit floating A, n, and E. The parameters are highly correlated and, therefore, the value of n (3.96) was rounded to 4 and fixed with A and E allowed to float and the errors in A and E represent the 95% confidence limits.

DISCUSSION

The excellent agreement for reaction (8) between this work, using different OH precursors, and the IUPAC recommendation and the good agreement with previous determinations for the kinetics of reaction (9) around ambient temperatures [33–35] confirms the validity of the technique to study a range of OH reactions.

The obvious major prerequisite of this method of OH generation is that the reaction must be studied in the presence of oxygen. Sufficient oxygen needs to be added to ensure that OH production from reaction (6a) is rapid compared to loss with the substrate and to prevent acetyl recombination. The exact concentrations of oxygen required will depend on the pseudo-first-order loss rates for the OH reaction with substrate; bimolecular rate coefficients for reaction (6) are pressure dependent [19] but are of the order (2–4) $\times 10^{-12}$ cm^3 $molecule^{-1}$ s^{-1} between 5 and 200 Torr of helium bath gas at room temperature and thus $[O_2]$ in region 10^{14}–10^{15} molecule cm^{-3} will give pseudo-first-order rate coefficients for growth of 200–4000 s^{-1} depending on $[O_2]$ and pressure. $[O_2] > 10^{16}$ molecule cm^{-3} will generally ensure that the growth of OH is so rapid that Eq. (E4) may be replaced by a simple single exponential analysis.

Two factors control the range of conditions that the ketone/oxygen system can be used as a practical OH

Table II Summary of Temperature-Dependent Parameterizations of k_{EtOH}

	k_{EtOH} (cm^3 $molecule^{-1}$ s^{-1})	
Precursor	Weighted by Statistical Error Only	Weighted by Statistical and Systematic Error
t-Butyl hydroperoxide	$(5.27 \pm 0.24) \times 10^{-18} T^2 \exp((557 \pm 20)\text{K}/T)$	$(5.7 \pm 3.4) \times 10^{-18} T^2 \exp((530 \pm 220)\text{K}/T)$
Acetone/O_2	$(5.87 \pm 0.34) \times 10^{-18} T^2 \exp((515 \pm 21)\text{K}/T)$	$(6.2 \pm 3.3) \times 10^{-18} T^2 \exp((500 \pm 200)\text{K}/T)$

Table III Summary of Results for the OH + MEK Reaction (R9)

T (K)	P (Torr)	k (10^{-12} cm^3 molecule^{-1} s^{-1})[a]	[MEK] (10^{14} molecule cm^{-3})	[O_2] (10^{16} molecules cm^{-3})	[OH]$_0$ (10^{11} molecules cm^{-3})	
213	25	0.93 ± 0.20	4.0–19.0	0.86	0.87–4.1	[b]
223	25	0.91 ± 0.04	2.7–24.6	0.91	0.5–4.5	[b]
248	41	0.98 ± 0.02	6.5–45.3	1.05	1.2–8.3	[b]
273	36	1.10 ± 0.07	5.9–28.3	1.20	1.9–7.6	[b]
285	31	0.98 ± 0.03	1.1–17.2	0.75	0.3–4.2	[b]
295	35	1.00 ± 0.09	4.0–19.0	0.64–0.73	1.4–5.5	[b]
298	25	1.06 ± 0.06	1.5–15	3.5	0.6–1.1	[c]
348	25	1.05 ± 0.02	1.3–12.1	3.6	0.34–3.2	[b]
398	25	1.36 ± 0.03	1.2–11	2.6	1.6–8.6	[c]
398	21	1.26 ± 0.13	3.0–17	2.6	2.4–8.6	[c]
398	503	1.44 ± 0.09	2.1–12	–	2.5–11	[c,d]
448	25	1.63 ± 0.05	1.4–14	4.0	0.8–8.0	[c]
498	25	1.83 ± 0.04	1.2–11	2.0	4.3–16	[c]
498	25	2.10 ± 0.25	1.5–8.5	3.7	0.9–5.0	[c]
498	25	1.97 ± 0.21	1.7–9.2	0.097	1.0–5.4	[c]
548	25	2.36 ± 0.06	0.94–8.0	1.9	0.8–6.6	[c]
598	25	2.48 ± 0.28	1.5–6.7	4.2	1.2–5.5	[c]

[a] Errors are 2σ statistical errors from the weighted linear fits of the pseudo-first-order rate coefficient vs. [MEK].
[b] Low temperature cell immersed in either heated (348 K) or cooled liquid.
[c] Resistively heated high-temperature cell.
[d] t-Butyl hydroperoxide used as the precursor.

source. The first is the competition between thermal decomposition of the acetyl radical and reaction with O_2, and this limits the upper temperature of study. The second is the competition between dissociation of the excited $RC(O)O_2^*$ complex to give OH and stabilization to give the relatively unreactive stabilized peroxy radical. This competition limits the upper pressure at which the system is a useful source of OH for kinetic studies.

Temperature

The main driver limiting the upper temperature range is decomposition of the RCO fragment. Acetyl decomposition has a strong positive temperature dependence [36] and above 700 K, more than 1×10^{17} molecule cm^{-3} of oxygen needs to be added to intercept the acetyl radicals. In theory, oxygen can be added up to the point when the total pressure is high enough to ensure sufficient OH formation from reaction (6a); however, if laser-induced fluorescence is used to probe [OH], fluorescence quenching by oxygen will reduce the OH signal due to fluorescence quenching. Reaction (9) has been studied up to 600 K in this work with [O_2] of 4.2×10^{16} molecule cm^{-3} (Table III). Above this temperature, fluorescence quenching by the amount of oxygen required to form OH prevented OH detection.

There are two minor temperature-dependent contributions. The rate coefficient for reaction (6) has a negative temperature dependence and thus even without acetyl decomposition, increasing concentrations of oxygen would be required to maintain the same pseudo-first-order rate coefficient for reaction (6) as temperature is increased. As the temperature increases, the yield of OH increases for a given bath gas concentration as the $RC(O)O_2^*$ complex is formed with increased energy [23] as shown in Fig. 7. This effect will partially compensate for the fluorescence quenching of the additional oxygen required to intercept acetyl formation at higher temperatures.

Pressure

Increasing pressure decreases the amount of OH formed from reaction (6a). At room temperature, the maximum pressure of helium at which sufficient OH signal could be observed for experimental kinetics was 200 Torr. Figure 7 shows how the yield of OH from reaction (6a) varies with temperature and pressure. In these experiments, the acetyl radical has been generated from acetone photolysis at 248 nm and the values have not been corrected for the pressure dependence of the CH_3CO yield as reported by Somnitz et al. [25].

The exact range of conditions for which the acetyl/O_2 reaction is a viable OH source will depend on the nature of the OH detection and the sensitivity of the particular apparatus. Figure 8 shows a plot where the OH yields from reaction (6a) have been mapped

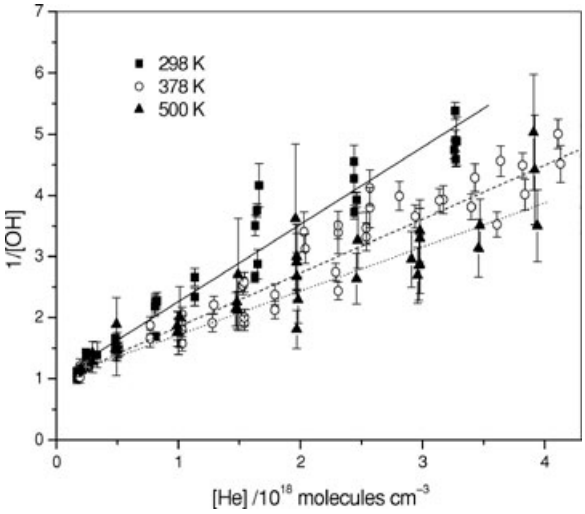

Figure 7 Stern Volmer plot for the OH yield from the acetyl + O_2 reaction at temperatures of 298–500 K.

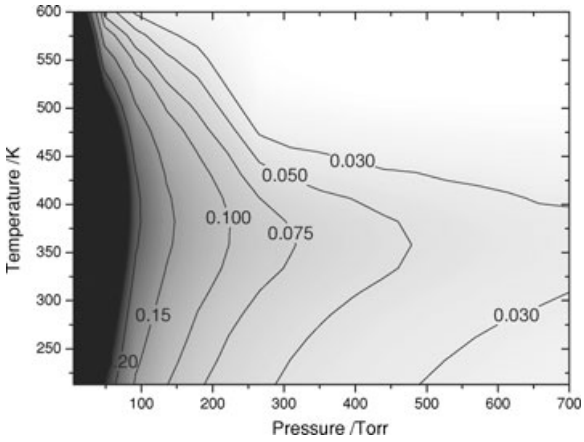

Figure 8 OH yields from reaction (6a) as a function of pressure and temperature for a fixed $[O_2] = 1 \times 10^{16}$ molecule cm^{-3}.

out as a function of pressure and temperature using a constant $[O_2] = 1 \times 10^{16}$ molecule cm^{-3}. The data for Fig. 8 come from Stern Volmer plots similar to those shown in Fig. 7 and from temperature-dependent rate coefficients for the decomposition of the acetyl radical taken from the evaluation of Baulch et al. [37].

Wavelength

Figure 1 shows that the acetone cross section extends into the near UV. At longer wavelengths, pressure quenching of the excited acetone species becomes significant and the quantum yield for CH_3CO decreases with temperature. The quantum yield of acetyl formation from acetone has recently been extensively studied as a function of temperature, pressure, and wavelength by Blitz et al. [26]. At long wavelengths (>300 nm), the Stern Volmer plots are nonlinear, indicating the possible involvement of multiple electronic states in the dissociation process. Sufficient OH was formed for kinetic studies of OH reactions out to 327 nm so that the acetone/O_2 system is a good OH source at relatively long wavelengths.

At wavelengths below approximately 270 nm, the acetyl radical can fragment via a unimolecular, and hence pressure-dependent, reaction to form the corresponding alkyl radical and CO.

Range of Ketones

A majority of the discussion has considered acetone to be the source of the RCO radical, but as our study on the reaction of OH with MEK, higher ketones can be used, too and OH signals have been observed from the photolysis of diethylketone at 248 nm in the presence of oxygen [23]. However, acetone is the best source; alternative photolysis pathways are minimal (e.g., H atom production) [38]. Only a single RCO fragment is formed, and it is the most thermally stable ketone and has the smallest rate coefficient for reaction with OH.

Comparison with Other OH Generation Methods

The prerequisite of a significant oxygen concentration has already been mentioned. For many studies, this will not be a problem and in some cases reactions are studied in a synthetic air mixture to mimic atmospheric conditions. However, in some cases the presence of oxygen can cause regeneration of OH radicals either in much the same way as OH is produced from reaction (6a) or by indirect secondary reactions. This limits the universal applicability of the technique.

Otherwise, the method has many advantages; the precursors are readily available in high purity and at low cost. Both oxygen and acetone are easy to handle although larger ketones can show unwanted wall effects at ambient and low temperatures. Acetone is relatively unreactive to OH with IUPAC [9] recommending a room temperature rate coefficient of $\sim 1.8 \times 10^{-13} cm^3$ $molecule^{-1}$ s^{-1}, slower than the corresponding reaction with ethane. The rate coefficient rises to $\sim 1.1 \times 10^{-12} cm^3$ $molecule^{-1}$ s^{-1} at 600 K [6]. Typically, with an unfocused 248 nm excimer operating at 10 mJ $pulse^{-1}$ and at pressures of less than 25 Torr, acetone concentrations of the order of 2×10^{13} molecule cm^{-3} are required to generate sufficient OH signal for our experiments. Under these conditions, the OH + acetone reaction contributes only 20 s^{-1} to the pseudo-first-order OH removal rate coefficient.

The method is particularly useful for OD isotope studies to investigate the kinetics and mechanisms of OH reactions. CD_3COCD_3 is readily available at low cost and with high isotopic purity, but importantly the strength and low polarity of the C–D bond means that exchange processes are unlikely as the gases are stored or delivered to the reaction cell. This is in contrast to precursors that directly produce OH(D) such as nitric acid, where the H(D) atom of the O—H(D) bond can readily exchange, and the storage vessels and delivery lines need to be passivated before reproducible data can be obtained. The kinetics of and OD yields from the reaction of $CD_3CO + O_2$ will be presented in a future paper.

Finally, the acetyl + O_2 reaction produces OH solely in the ground vibrational state. After tuning up the probe laser to detect OH ($v = 1$) from the Q branch of the $A^2\Sigma(v = 2) \leftarrow X^2\Pi(v = 1)$ transition around 289 nm via reaction (10) [39]

$$H + NO_2 \rightarrow OH(v = 2, 1, 0) + NO \qquad (10)$$

with H atoms being generated from the photolysis of H_2S at 248 nm, we were unable to observe any OH ($v = 1$) from the acetyl + O_2 reaction. Allowing for the reduced sensitivity of the dye laser in this region of spectrum, our inability to observe any vibrationally excited OH puts an upper limit of 7% on the production of OH ($v = 1$). The absence of any vibrationally excited OH is consistent with our current understanding of the mechanism of the reaction. An ab initio calculation shows that the initial coproduct is the three-membered lactone with an exothermicity of $\sim$130 kJ mol^{-1} [21]. It is possible that a highly dynamically constrained dissociation of the intermediate to give OH + lactone could partition approximately one third of the exothermicity into the OH radical sufficient to vibrationally excite the OH molecule. However, it is more likely that that energy will be partitioned statistically within the complex and hence that the lactone with its far greater number of low-frequency vibrational modes will take most of the energy and OH will be formed in its vibrational ground state.

We are grateful to NERC for a studentship for BJSP.

BIBLIOGRAPHY

1. Heard, D. E.; Pilling, M. J. Chem Rev 2003, 103, 5163–5198.
2. Walker, R. W.; Morley, C. In Low Temperature Combustion and Autoignition; Pilling, M. J. (ed.); Elsevier: Amsterdam, 1997; pp. 1–124.
3. Saunders, S. M.; Jenkin, M. E.; Derwent, R. G.; Pilling, M. J. Atmos Chem Phys 2003, 3, 161–180.
4. August, J.; Brouard, M.; Docker, M. P.; Milne, C. J.; Simons, J. P.; Lavi, R.; Rosenwaks, S.; Schwartzlavi, D. J Phys Chem 1988, 92, 5485–5491.
5. Vaghjiani, G. L.; Ravishankara, A. R. J Chem Phys 1990, 92, 996–1003.
6. Yamada, T.; Taylor, P. H.; Goumri, A.; Marshall, P. J Chem Phys 2003, 119, 10600–10606.
7. Talukdar, R. K.; Gierczak, T.; McCabe, D. C.; Ravishankara, A. R. J Phys Chem A 2003, 107, 5021–5032.
8. Wollenhaupt, M.; Carl, S. A.; Horowitz, A.; Crowley, J. N. J Phys Chem A 2000, 104, 2695–2705.
9. IUPAC. IUPAC Subcommittee for Gas Kinetic Data Evaluation, 2007.
10. McCabe, D. C.; Brown, S. S.; Gilles, M. K.; Talukdar, R. K.; Smith, I. W. M.; Ravishankara, A. R. J Phys Chem A 2003, 107, 7762–7769.
11. Smith, I. W. M. J Chem Soc, Faraday Trans 1997, 93, 3741.
12. Okabe, H. Photochemistry of Small Molecules; Wiley: New York, 1988.
13. Gericke, K. H.; Comes, F. J.; Levine, R. D. J Chem Phys 1981, 74, 6106–6112.
14. Silvente, E.; Richter, R. C.; Hynes, A. J. J Chem Soc, Faraday Trans 1997, 93, 2821–2830.
15. D'Ottone, L.; Bauer, D.; Campuzano-Jost, P.; Fardy, M.; Hynes, A. J. Phys Chem Chem Phys 2004, 6, 4276–4282.
16. Yamasaki, K.; Watanabe, A.; Kakuda, T.; Tokue, I. J Phys Chem A 2000, 104, 9081–9086.
17. Michael, J. V.; Keil, D. G.; Klemm, R. B. J Chem Phys 1985, 83, 1630–1636.
18. Tyndall, G. S.; Orlando, J. J.; Wallington, T. J.; Hurley, M. D. Int J Chem Kinet 1997, 29, 655–663.
19. Blitz, M. A.; Heard, D. E.; Pilling, M. J. Chem Phys Lett 2002, 365, 374–379.
20. Devolder, P.; Dusanter, S.; Lemoine, B.; Fittschen, C. Chem Phys Lett 2005, 417, 154–158.
21. Baeza Romero, M. T.; Blitz, M. A.; Heard, D. E.; Pilling, M. J.; Price, B.; Seakins, P. W.; Wang, L. Faraday Discuss 2005, 130, 79–87.
22. Ravishankara, A. R. Personal Communication, 2006.
23. Baeza Romero, M. T.; Blitz, M. A.; Heard, D. E.; Pilling, M. J.; Price, B.; Seakins, P. W. Chem Phys Lett 2005, 408, 232–236.
24. Woodbridge, E. L.; Fletcher, T. R.; Leone, S. R. J Phys Chem 1988, 92, 5387–5393.
25. Somnitz, H.; Fida, M.; Ufer, T.; Zellner, R. Phys Chem Chem Phys 2005, 7, 3342–3352.
26. Blitz, M. A.; Heard, D. E.; Pilling, M. J. J Phys Chem A 2006, 110, 6742–6756.
27. Anastasi, C.; Smith, I. W. M.; Parkes, D. A. J Chem Soc, Faraday Trans 1 1978, 74, 1693–1701.
28. Hess, W. P.; Tully, F. P. Chem Phys Lett 1988, 152, 183–189.

29. IUPAC. IUPAC Subcommittee for Gas Kinetic Data Evaluation, 2006.
30. Wallington, T. J.; Kurylo, M. J. Int J Chem Kinet 1987, 19, 1015–1019.
31. Jimenez, E.; Gilles, M. K.; Ravishankara, A. R. J Photochem Photobiol A: Chem 2003, 157, 237–243.
32. Dillon, T. J.; Holscher, D.; Sivakumaran, V.; Horowitz, A.; Crowley, J. N. Phys Chem Chem Phys 2005, 7, 349–354.
33. Jimenez, E.; Ballesteros, B.; Martinez, E.; Albaladejo, J. Environ Sci Technol 2005, 39, 814–820.
34. Wallington, T. J.; Kurylo, M. J. J Phys Chem 1987, 91, 5050–5054.
35. Le Calve, S.; Hitier, D.; Le Bras, G.; Mellouki, A. J Phys Chem A 1998, 102, 4579–4584.
36. Bencsura, A.; Knyazev, V. D.; Slagle, I. R.; Gutman, D.; Tsang, W. Ber Bunsen-Ges Phys Chem 1992, 96, 1338–1347.
37. Baulch, D. L.; Cobos, C. J.; Cox, R. A.; Frank, P.; Hayman, G.; Just, T.; Kerr, J. A.; Murrells, T.; Pilling, M. J.; Troe, J.; Walker, R. W.; Warnatz, J. J Phys Chem Ref Data 1994, 23, 847–1033.
38. Lightfoot, P. D.; Kirwan, S. P.; Pilling, M. J. J Phys Chem 1988, 92, 4938–4946.
39. Irvine, A. M. L.; Smith, I. W. M.; Tuckett, R. P.; Yang, X. F. J Chem Phys 1990, 93, 3177–3186.